Research Article | Vol. 30, No. 21 / 10 Oct 2022 / Optics Express 38966
Optics EXPRESS

# Mach-Zehnder interferometer based fiber-optic nitrate sensor

ABDULLAH AL NOMAN,[1] JITENDRA NARAYAN DASH,[2] XIN CHENG,[2,*] HWA-YAM TAM,[2] AND CHANGYUAN YU[1,3]

[1] *Photonics Research Center, Department of Electronic and Information Engineering, The Hong Kong Polytechnic University,11 Yuk Choi Rd., Hung Hom, Hong Kong SAR, China*
[2] *Photonics Research Center, Department of Electrical Engineering, The Hong Kong Polytechnic University, 11 Yuk Choi Rd., Hung Hom, Hong Kong SAR, China*
[3] *changyuan.yu@polyu.edu.hk*
[*] *eechengx@polyu.edu.hk*

**Abstract:** A biocompatible, reliable and quick responsive fiber-optic sensor based on Mach-Zehnder interferometer (MZI) is demonstrated for nitrate analytes tracing. The sensor was constructed by collapsing the air holes of a short length photonic crystal fiber (PCF) with the single-mode fibers (SMFs) on both ways. The proposed sensor has been coated with a graphene-PVA (polyvinyl alcohol) membrane using the thermal coating technique to make the sensor attractive to the nitrate ions in the aqueous solution. The maximum response is found to be 0.15 pm/ppm on the nitrate measurement scale of 0 ppm to 100 ppm with an average reaction time of ~10 s. Also, a short length of FBG (fiber Bragg grating) is implanted with SMF to improve the sensing accuracy of the presented sensor.



## 1. Introduction

Nitrate ($NO_3^-$) is a typical compound found in the environment due to its diverse applications (e.g., accelerating plant growth, human health enhancement, food preservation) [1–3]. Over the long term, it has appeared to be a contaminant of water pollution as its usage has been increased in industry, agriculture and food processing [4,5]. Moreover, the high concentration of nitrate ions can endanger the aquatic ecosystem and human health. In particular, excessive nitrate substances reduce the oxygen-carrying mechanism capacity in the human blood which in turn creates methemoglobin disease [6,7]. Therefore, WHO (World Health Organization) and other environmental organizations have set the tolerance point for nitrate concentration in drinking water up to 50 ppm (parts per million) (equivalent to 10 ppm nitrate-nitrogen) [3,4,8]. Besides, numerous scientific method-based sensors have been applied to determine the nitrate quantity level, such as chromatography, electrochemical, spectroscopy and electrophoresis [9–12]. However, these techniques are constricted to the convoluted fabrication process, require pricey instruments, and take an extended detection period [13,14].

Meantime, fiber-optic based sensors present more benefits over the typical systems; for instance: resistance to electromagnetic signals, small in size, highly accurate and less expensive [15–18]. To date, diverse optical approaches have been exhibited for nitrate compound confirmation in water. For example, a polymeric layer (poly(3,4-ethylenedioxythiophene) (PEDOT)) coated at the tip of single-mode fiber (SMF) has been reported for nitrate detection, where a linear response was observed in-between 0.2 ppm – 40 ppm with a limit of detection (LOD) of 6.7 ppm [8]. Moreover, a similar structure was followed using a graphene layer [14]. The coating was overlayed using a dip-casting method and immersed into the nitrate concentrations from 0 ppm to 50 ppm to achieve a sensitivity of 0.0624 dBm/ppm. Also, a multimode fiber (MMF) coated with lophine membrane (2,4,5-Triphenylimidazol) was demonstrated to detect similar substances [13]. The sensor was tested in the nitrate solution range from 1 ppm to 70 ppm with a response

#468944 https://doi.org/10.1364/OE.468944
Journal © 2022 Received 26 Jun 2022; revised 11 Aug 2022; accepted 17 Aug 2022; published 6 Oct 2022

Optics EXPRESS

time of 20 ms – 40 ms. Fiber-optic based SPR (surface plasmon resonance) sensor has also been presented towards nitrate identification by applying carbon nanotubes (CNT) membrane [4]. On the contrary, interferometric based fiber sensors have gained interest for nitrate tracing due to their advantages (e.g., short response period, high sensitivity, simple assembly process) [19,20]. A microfiber modal cavity (MMC) based fiber device has been designed to measure the nitrate concentration between 0 ppm to 1470 ppm [21]. The sensor has shown a sensitivity of 5.98 pm/ppm by considering a broader measurement range. Nevertheless, the application of these sensors are limited due to several complexities, such as complicated chemical processes, confined to small-scale detection, longer response times and less sensitivity to nitrate ions.

Graphene is a broadly interested two-dimensional (2D) material across numerous disciplines due to its excellent thermal properties, both electrically and mechanically [22,23]. The single layer of carbon structure in graphene allows tremendous conductivity, chemical inertness, low resistivity and high surface area, making them engage in biochemical sensing [24]. Also, the eco-friendly properties in graphene allow them to apply in various applications (e.g., medicine [25], human health monitoring [26] and food safety [27]). Conversely, polyvinyl alcohol (PVA) is a water immersible polymeric substance which diversely used in chemical fiber, medicine and food production [28]. Besides, PVA offers several qualities such as biocompatibility, good chemical stability and cohesive properties with optical fiber [29]. Also, PVA has been immensely used in fiber sensing applications to improve the attachment capability on silica fiber surface through its aqua soluble synthetic polymer [28,30–32].

The aim of this investigation is to demonstrate a compact and high sensitive fiber-optic Mach-Zehnder interferometric sensor for nitrate ion detection. The transmission based cavity has been formulated by splicing SMF on both sides of a small photonic crystal fiber (PCF) length. The sensor is coated with graphene and PVA mixed solution to make it receptive towards nitrate ions. The response of the sensor towards minute change in nitrate concentration has been studied along with temperature response and response time. The selectivity of the sensor is also analyzed to improve the sensor accuracy. Additionally, fiber Bragg grating (FBG) has been utilized along with the MZI to monitor error in measurement due to cross temperature sensitivity.

## 2. Materials and sensor fabrication

### 2.1. Reagents

Sulfuric acid (99%), acetic acid (99%), (3-Aminopropyl)triethoxysilane (APTES, 97%), potassium dichromate, PVA (99%), ethanol, sodium nitrate and sodium chloride were obtained from Sigma Aldrich. Copper sulfate pentahydrate (99%) was purchased from Aladdin. Besides, graphene dispersed water was bought from XFNANO. All of these reagents were of the highest analytical grade. Furthermore, different nitrate and other anion concentrations have been made through the dilution process with deionized water (DI).

### 2.2. Preparation of fiber sensor

The fiber-optic interferometric sensor was constructed by applying a sandwich structure (shown in Fig. 1), where a 12 mm length of commercial PCF (Newport, model no: F-SM8) was sandwiched between two single-mode fibers (SMFs) through a commercial fusion splicer (FITEL s178A). Thus, the spliced region of SMF-PCF collapsed the PCF air holes over about 290 µm in length (see Fig. 2(b)) due to the adjustable arc discharge of the splicer. The geometry of the presented PCF is depicted in Fig. 2(a), along with the pitch ($\Lambda$) and diameter (d) of the PCF air holes. Moreover, the median core diameter of PCF, the pitch and diameter of air holes in PCF are 8.6 µm, 5.63 µm and 2.39 µm, respectively. Also, a piece of FBG was embedded into the SMF with a length and pitch of 5 mm and 0.53 µm, which was combined prior to the SMF-PCF collapsed area.

Optics EXPRESS

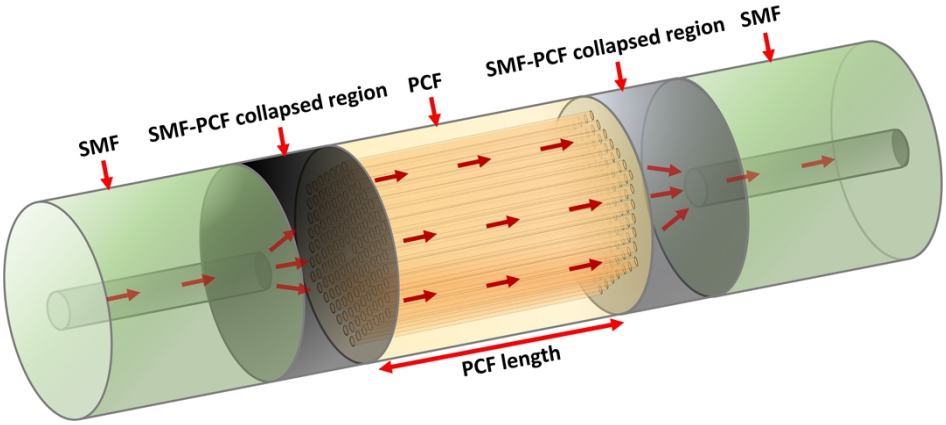


**Fig. 1.** Schematic of MZI based fiber-optic nitrate sensor.

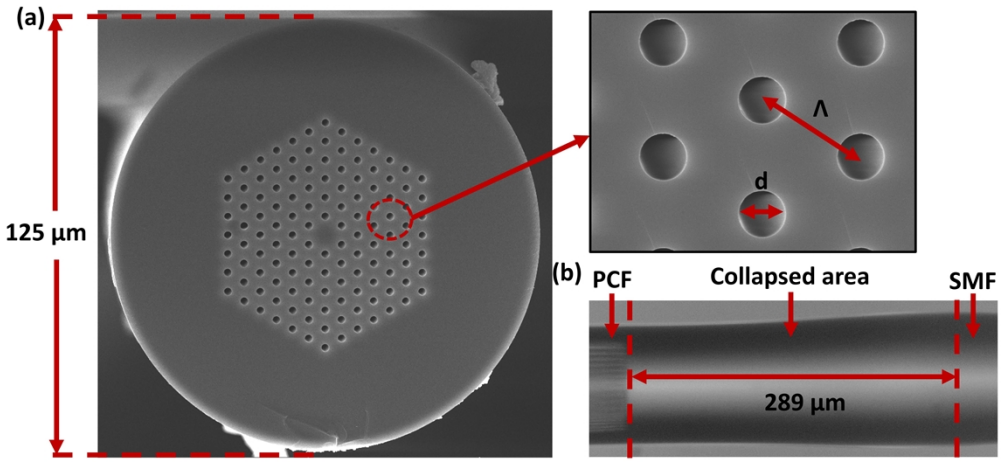


**Fig. 2.** (a) Cross-sectional image of PCF with pitch and diameter of air holes (inset), (b) collapsed area of SMF and PCF.

The prepared probe was then functionalized to deposit the sensing membrane [33]. In this process, the fiber was submerged into the sulfochromic solution (1 mg of potassium dichromate and 0.1 ml of DI water added to 10 ml of sulfuric acid) for 10 min at ambient temperature, followed by DI water wash to produce hydroxyl bonds (-OH) on the PCF surface. The probe was dried at 110°C for two hours in the oven. Thereafter, the probe was treated with the amino-saline solution for 3–5 min in an Argon gas environment and bathed in ethanol solution. The saline concoction was made by mixing 1% APTES into acetic acid and ethanol (4:10, v/v) solution, where the existence of acetic acid helps to prevent the multi-layers saline structure. The probe was again dehydrated at 110°C for two hours to enrich the stability. This process creates the amino groups on the PCF surface to assist in making bonding with deposited sensing materials, as illustrated in Fig. 3(a). Afterwards, the functionalized probe was coated with graphene/PVA film through the thermal coating at 90°C for two hours. The graphene and PVA solution was prepared by mixing 1 g/L of graphene disperse solvent and 1 g/L of PVA in a ratio of 2:1 (v/v). Moreover, the scanning electron microscope (SEM) image of the coated probe has shown in

Optics EXPRESS

Fig. 3(b) to validate the graphene layer. A similar approach was followed to make three probes to ensure the duplicability of the sensor towards nitrate analytes.

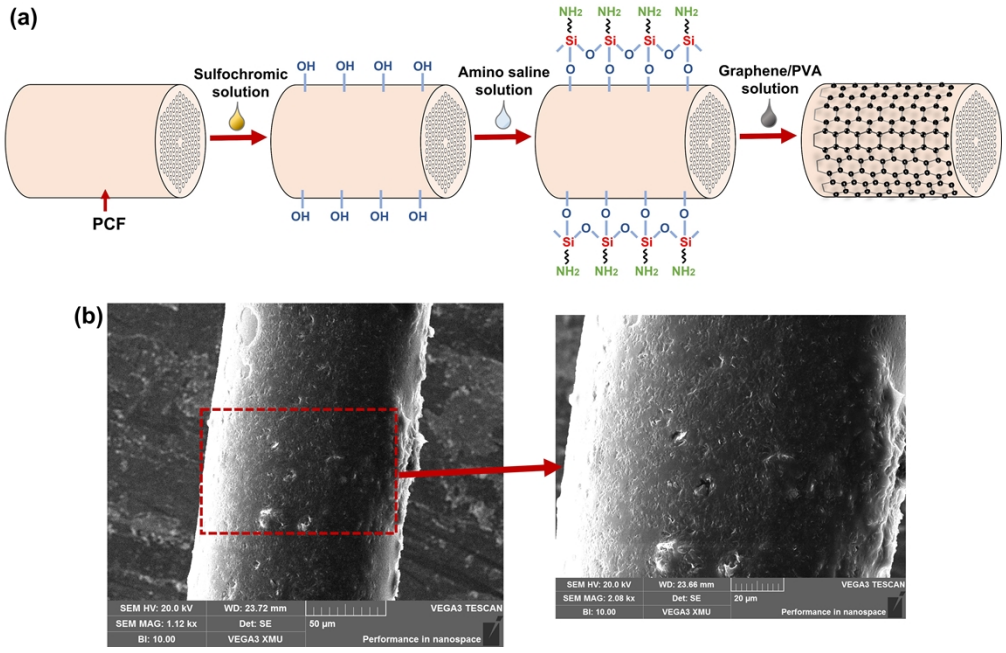


**Fig. 3.** (a) Functionalized process for the fabricated interferometric fiber sensors, (b) SEM image of the coated probe.

## 3. Sensing principle and experimental setup

### 3.1. Principle analysis

The light distribution of the proposed sensor is displayed in Fig. 1. When the light is launched into the fiber, the fundamental mode of SMF gets diffracted at the SMF-PCF collapsed region which in turn simultaneously excites both the core and cladding modes in PCF. Further, these modes propagate along the PCF and consolidate again at the second SMF-PCF junction, and ultimately gets filtered through the SMF. Besides, there is a phase difference between the core and cladding mode due to different propagation constants and the total intensity of the resultant interference pattern can be expressed as [34]:

$$I_t = I_1 + I_2 + 2\sqrt{I_1 I_2}\cos\left(\frac{2\pi(n_{core} - n_{claddiing})L}{\lambda}\right) \tag{1}$$

where, $I_1$ and $I_2$ refers to the intensity of light in core and cladding of PCF, respectively, while $n_{core}$ and $n_{cladding}$ represents the refractive index (RI) of core and cladding respectively, $L$ is the PCF length and λ is the utilized wavelength. The sensing principle relies on the interaction of the evanescent wave of cladding modes of PCF with the adjacent environment. Hence, change in the RI of the nearby medium affects the effective index of cladding modes, leading to the movement in the interference to form total spectra.

### 3.2. Experimental procedures

The experimental arrangement for the MZI based nitrate sensor is illustrated in Fig. 4(a). The setup involves a homemade broadband source (BBS, with a maximum output power of 3 mW),

Optics EXPRESS

a fabricated probe and an optical spectrum analyzer (OSA, AQ6370D, YOKOGAWA, Tokyo, Japan). Light is launched into the fiber from the BBS and the resulting cladding modes in PCF interacts with the ambient environment and ultimately gets collected by SMF which in turn is connected to OSA. Figure 4(b) displays the produced interference pattern by following the above arrangement, which corresponds to the earlier and later coating state of the fabricated probe while the sensor was out of the solution. Further, upon graphene/PVA deposition, a variation has been noticed both in intensity and interference dip as a consequence of the interaction of the evanescent field of cladding mode with the graphene/PVA composite. Besides, the sharp dip (see Fig. 4(b)) generated in the spectra refers to the presence of FBG in the SMF.

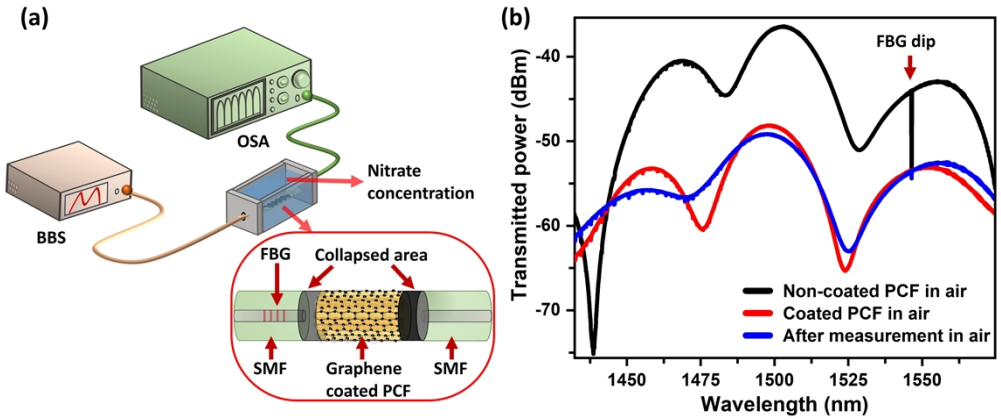


**Fig. 4.** (a) Experimental setup for the proposed nitrate sensor, (b) interference pattern of the sensor before and after coating sensing membrane.

## 4. Results & discussion

The sensor sensitivity for nitrate analytes was recorded by utilizing the presented experimental setup, where the sensor was immersed in solutions with various nitrate concentrations varying from 0 ppm to 100 ppm. As can be noticed from Fig. 5(a), the interference minima showed a red shift upon submersion into the nitrate solution. The redshift can be attributed to the attachment of nitrate ions with graphene leading to the change in the effective index of cladding modes of PCF [35,36]. Additionally, three probes were fabricated with similar geometrical parameters of PCF and coating procedures to authenticate the accuracy of reproducibility. The average sensitivity for these probes was calculated by considering the above process for three turns, where the normalized sensitivity for nitrate detection was found to be 13.5 pm/ppm, 13 pm/ppm and 15 pm/ppm (displayed in Fig. 5(b)). Besides, the LOD was recorded as 3.33 ppm taking into account the maximum sensitivity among the probes and the spectral resolution of OSA (resolution = 0.05 nm). Furthermore, these probes can be reusable as initial spectra remain unchanged after each measurement while the probe was out of the nitrate solution (see Fig. 4(b)).

Subsequently, the response time of the proposed probe concerning different nitrate concentrations was analyzed using an interrogator (SM125, MICRON OPTICS). In this continuum, the sensor was dipped into three different nitrate solutions (20 ppm, 60 ppm and 100 ppm), as presented in Fig. 6(a). The response time was found to be 11 s and 9.5 s during the transition of the sensor from 20 ppm to 60 ppm and 60 ppm to 100 ppm, respectively (see Fig. 6(b) and 6(c)). While in inverse order, a similar reaction period can be observed in Fig. 6(d) and 6(e). In the aqueous solutions, the instant attachment of nitrate ions with graphene led to the instantaneous shift in spectra which in turn resulted in a quick response. The measured average reaction time

Optics EXPRESS

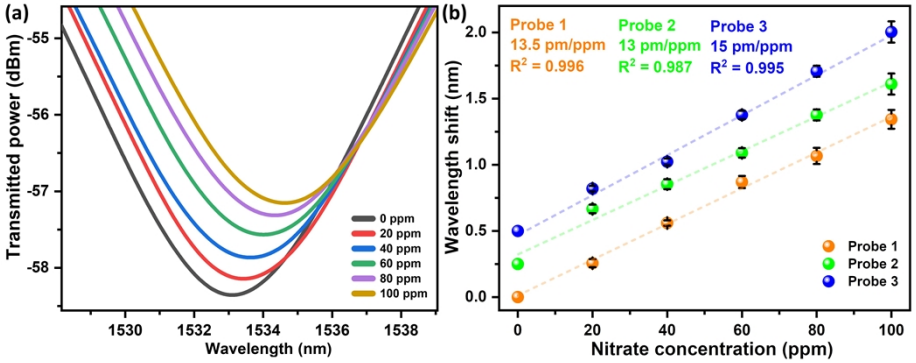


**Fig. 5.** (a) Movement in the interference minima for the various nitrate concentrations (probe 3), (b) average sensitivity of the three fabricated probes towards nitrate detection.

(about 10 s) was discovered to be better in comparison with the existing fiber sensor [8] and the measurement scale is broader compared to the previous reports [1,4,13,14]. Additionally, the performance of the various optical fiber based sensors for nitrate identification was reviewed in Table 1.

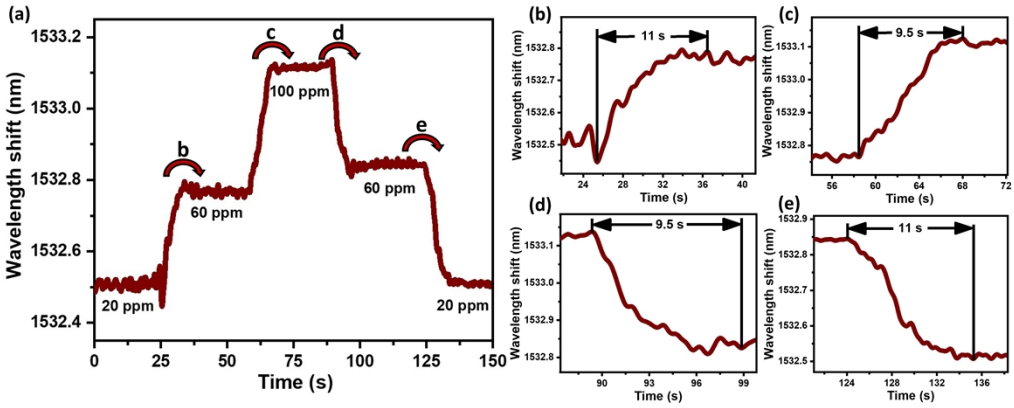


**Fig. 6.** (a) Response time of the proposed sensor between 20 ppm, 60 ppm and 100 ppm of nitrate mixture. (b), (c), (d) and (e) are the inset which refers to the following transition state: 20 ppm to 60 ppm, 60 ppm to 100 ppm, 100 ppm to 60 ppm and 60 ppm to 20 ppm, respectively.

The response of the fabricated nitrate sensor has further been investigated to confirm its selectivity towards other anion solutions. Two anion solutions chloride ($Cl^-$) and sulfate ($SO_4^{2-}$) with a concentration range varying from 0 ppm to 100 ppm were considered for selectivity verification. It can be observed from Fig. 7 that the sensor was nearly five times more responsive to nitrate substances than the other bases. This can be attributed to the affinity of the nitrate ions with graphene.

Monitoring the response of the sensor to the change in ambient environmental temperature is an essential requirement that has been investigated in this study, considering the dip corresponding to interference minima as well as FBG. Following this approach, the sensor was kept inside a temperature furnace and the temperature was varied from 25°C to 45°C at a step of 5°C. The inset in Fig. 8(a) and 8(b) displays a redshift of the interference as well as FBG spectra, and the corresponding linear response can be seen in Fig. 8(a) and 8(b). The temperature sensitivity for

Optics EXPRESS

**Table 1. Performance of the numerous fiber sensors for nitrate detection**

| Formation of sensors | Deposited material | Fabrication complexity | Measurement scale | Sensitivity | Response period | Ref. |
|---|---|---|---|---|---|---|
| Etched FBG based SMF | - | Simple | 0 ppm – 80 ppm | 3.5 pm/ppm | - | [1] |
| SPR based MMF | CNT | Complex | 0.160 ppm – 62 ppm | 0.44 nm/ppm | - | [4] |
| Reflection based fiber tip | PEDOT | Complex | 0.2 ppm – 40 ppm | 0.16 μW/ppm | 2 min | [8] |
| Transmission based MMF | Lophine | Complex | 1 ppm – 70 ppm | - | 20 ms – 40 ms | [13] |
| Reflection based fiber tip | Graphene | Simple | 0 ppm – 50 ppm | 0.0624 dBm/ppm | - | [14] |
| MZI based fiber sensor | Graphene | Medium | 0 ppm – 100 ppm | 15 pm/ppm | 9.5 s – 11 s | This study |

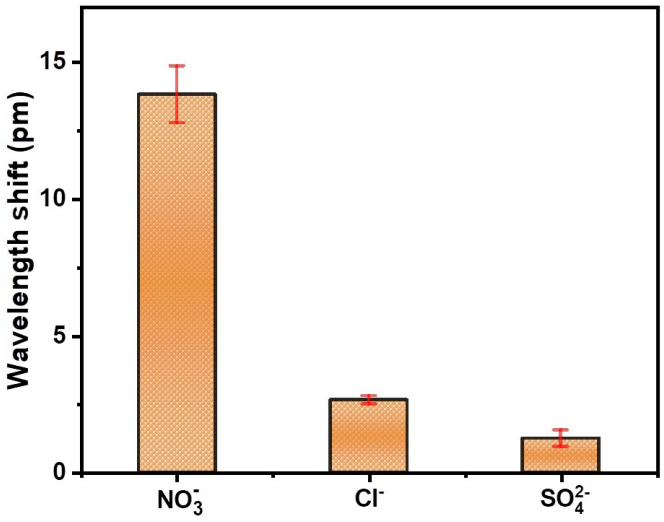


**Fig. 7.** Selectivity of the sensor with other bases.

the interferometric sensor was calculated to be 22.2 pm/°C, while that for FBG was found to be 19.4 pm/°C. Considering the response of MZI spectra to the change in nitrate ion concentration and environmental temperature, the cross-sensitivity was found to be 1.48 ppm/°C. The use of FBG with the interferometer assists in simultaneous measurement of temperature, thereby helping in the elimination of error in nitrate ion concentration measurement due to cross temperature effect.

Optics EXPRESS

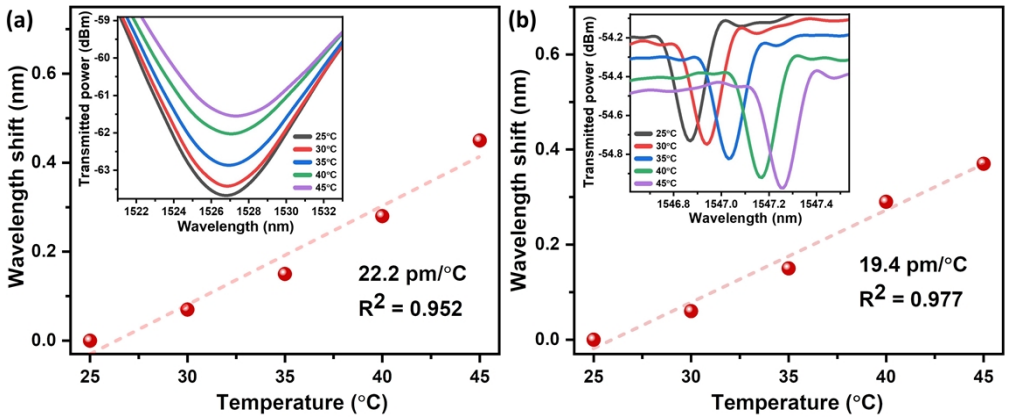


**Fig. 8.** Temperature response of both fiber optic interferometric sensor (a) and FBG (b).

## 5. Conclusion

A simple and quick reactive graphene and PVA layer coated fiber optic sensor has been presented for nitrate detection using MZI phenomena. The interferometric sensor was fabricated by splicing two SMFs on both sides of a small part of the PCF hexagonal shape. The probe went through a functionalization procedure followed by a thermally coating technique to apply the graphene-PVA layer. A similar tactic was used to make three different probes to ensure reproducibility, where among them the highest response was found to be 15 pm/ppm for the various concentrations of nitrate. The sensors were considered for nitrate measurement scale 0 ppm to 100 ppm at an interval of 20 ppm, where the standard reaction time of around 10 s has taken by the probe to detect nitrate substances in water. Furthermore, the sensor found to be more sensitive to nitrates than other anions. Besides, the minima in the spectra were traced to calculate the temperature response for both the interferometer based fiber sensor and FBG. The thermal sensitivity for MZI and FBG have been found to be 22.2 pm/°C and 19.4 pm/°C. Thus, the authentic response of the sensor towards nitrate can be accomplished by considering the cross-temperature sensitivity. These promising outcomes from the proposed MZI sensor can certainly be applicable for nitrate detection in the natural environment.

**Funding.** Research Grants Council, General Research Fund (15211317).

**Disclosures.** The authors declare no conflicts of interest.

**Data availability.** No data were generated or analyzed in the presented research.

## References

1. T. B. Pham, H. Bui, H. T. Le, and V. H. Pham, "Characteristics of the fiber laser sensor system based on etched-Bragg grating sensing probe for determination of the low nitrate concentration in water," Sensors **17**(12), 7 (2016).
2. J. O. Lundberg, E. Weitzberg, J. A. Cole, and N. Benjamin, "Nitrate, bacteria and human health," Nat. Rev. Microbiol. **2**(7), 593–602 (2004).
3. W. H. Organization, "Nitrate and nitrite in drinking-water: Background document for development of WHO Guidelines for Drinking-water Quality," (World Health Organization, 2003).
4. Y.-N. Zhang, E. Siyu, B. Tao, Q. Wu, and B. Han, "Reflective SPR sensor for simultaneous measurement of nitrate concentration and temperature," IEEE Trans. Instrum. Meas. **68**(11), 4566–4574 (2019).
5. M. Nehir, M. Esposito, C. Begler, C. Frank, O. Zielinski, and E. P. Achterberg, "Improved Calibration and Data Processing Procedures of OPUS Optical Sensor for High-Resolution in situ Monitoring of Nitrate in Seawater," (2021).
6. D. Pooja, P. Kumar, P. Singh, and S. Patil, *Sensors in water pollutants monitoring: role of material* (Springer, 2020).
7. B. Mahieuxe, M. Carré, M. Viriot, J. André, and M. Donner, "Fiber-optic fluorescing sensors for nitrate and nitrite detection," J. Fluoresc. **4**(1), 7–10 (1994).

Optics EXPRESS


8. S. Shahnia, H. Ebendorff-Heidepriem, D. Evans, and S. Afshar, "A fibre-optic platform for sensing nitrate using conducting polymers," Sensors **21**(1), 138 (2020).
9. E. Murray, P. Roche, M. Briet, B. Moore, A. Morrin, D. Diamond, and B. Paull, "Fully automated, low-cost ion chromatography system for in-situ analysis of nitrite and nitrate in natural waters," Talanta **216**, 120955 (2020).
10. B. R. Kozub, N. V. Rees, and R. G. Compton, "Electrochemical determination of nitrite at a bare glassy carbon electrode; why chemically modify electrodes?" Sens. Actuators, B **143**(2), 539–546 (2010).
11. K. A. Vakilian and J. Massah, "A portable nitrate biosensing device using electrochemistry and spectroscopy," IEEE Sens. J. **18**(8), 3080–3089 (2018).
12. I. S. da Silva, W. R. de Araujo, T. R. Paixão, and L. Angnes, "Direct nitrate sensing in water using an array of copper-microelectrodes from flat flexible cables," Sens. Actuators, B **188**, 94–98 (2013).
13. J. Camas-Anzueto, A. Aguilar-Castillejos, J. Castañón-González, M. Lujpán-Hidalgo, H. H. De Leon, and R. M. Grajales, "Fiber sensor based on Lophine sensitive layer for nitrate detection in drinking water," Opt. Lasers Eng. **60**, 38–43 (2014).
14. P. Ja'Afar, N. Razali, N. Zaidi, F. Ahmad, M. Omar, A. Ismail, N. Rosdi, M. Yaacob, A. Hamzah, and H. Kaidi, "Graphene coated optical fiber tip sensor for nitrate sensing application," in *2020 IEEE 8th International Conference on Photonics (ICP)*, (IEEE, 2020), 3–4.
15. A. Al Noman, J. N. Dash, X. Cheng, C. Y. Leong, H.-Y. Tam, and C. Yu, "Hydrogel based Fabry-Pérot cavity for a pH sensor," Opt. Express **28**(26), 39640–39648 (2020).
16. A. Al Noman, J. N. Dash, X. Cheng, and C. Yu, "Fiber optic lead ion (Pb2+) sensor using chitosan diaphragm based Fabry-Pérot interferometer," in *Optoelectronics and Communications Conference*, (Optical Society of America, 2021), W3D. 2.
17. M. A. M. Johari, A. Al Noman, M. A. Khudus, M. H. Jali, H. H. M. Yusof, S. W. Harun, and M. Yasin, "Microbottle resonator for formaldehyde liquid sensing," Optik **173**, 180–184 (2018).
18. M. A. M. Johari, M. I. M. A. Khudus, M. H. B. Jali, A. Al Noman, and S. W. Harun, "Effect of size on single and double optical microbottle resonator humidity sensors," Sens. Actuators, A **284**, 286–291 (2018).
19. A. Al Noman, J. N. Dash, X. Cheng, H.-Y. Tam, and C. Yu, "PCF based modal interferometer for lead ion detection," Opt. Express **30**(4), 4895–4904 (2022).
20. X. Cheng, J. N. Dash, D. S. Gunawardena, L. Hetien, and H. Tam, "Silicone Rubber Based Highly Sensitive Fiber-Optic Fabry–Perot Interferometric Gas Pressure Sensor," Sensors **20**(17), 4927 (2020).
21. L. Yang, J. Wang, S. Wang, Y. Liao, and Y. Li, "A new method to improve the sensitivity of nitrate concentration measurement in seawater based on dispersion turning point," Optik **205**, 164202 (2020).
22. C. H. Lu, H. H. Yang, C. L. Zhu, X. Chen, and G. N. Chen, "A graphene platform for sensing biomolecules," Angew. Chem. **121**(26), 4879–4881 (2009).
23. Y. Liu, X. Dong, and P. Chen, "Biological and chemical sensors based on graphene materials," Chem. Soc. Rev. **41**(6), 2283–2307 (2012).
24. N. A. A. Kadir, N. Irawati, A. A. A. Jafry, N. M. Razali, A. Hamzah, and S. W. Harun, "Sodium nitrate sensor based on D-shaped fiber structure," Measurement **163**, 107927 (2020).
25. S. Priyadarsini, S. Mohanty, S. Mukherjee, S. Basu, and M. Mishra, "Graphene and graphene oxide as nanomaterials for medicine and biology application," J. Nanostructure Chem. **8**(2), 123–137 (2018).
26. H. Huang, S. Su, N. Wu, H. Wan, S. Wan, H. Bi, and L. Sun, "Graphene-based sensors for human health monitoring," Front. Chem. **7**, 399 (2019).
27. A. K. Sundramoorthy and S. Gunasekaran, "Applications of graphene in quality assurance and safety of food," TrAC, Trends Anal. Chem. **60**, 36–53 (2014).
28. J. Li, X. Liu, H. Sun, L. Wang, J. Zhang, L. Deng, and T. Ma, "An optical fiber sensor coated with electrospinning polyvinyl alcohol/carbon nanotubes composite film," Sensors **20**(23), 6996 (2020).
29. H. Tian, J. Yan, A. V. Rajulu, A. Xiang, and X. Luo, "Fabrication and properties of polyvinyl alcohol/starch blend films: Effect of composition and humidity," Int. J. Biol. Macromol. **96**, 518–523 (2017).
30. C. Shao, H.-Y. Kim, J. Gong, B. Ding, D.-R. Lee, and S.-J. Park, "Fiber mats of poly (vinyl alcohol)/silica composite via electrospinning," Mater. Lett. **57**(9-10), 1579–1584 (2003).
31. Q. F. Ma, Z. Q. Tou, K. Ni, Y. Y. Lim, Y. F. Lin, Y. R. Wang, M. H. Zhou, F. F. Shi, L. Niu, and X. Y. Dong, "Carbon-nanotube/Polyvinyl alcohol coated thin core fiber sensor for humidity measurement," Sens. Actuators, B **257**, 800–806 (2018).
32. H. A. Zain, M. Batumalay, S. W. Harun, Z. Harith, M. Yasin, and H. R. A. Rahim, "Graphene/PVA coated D-shaped fiber for sodium nitrate sensing," Sens. Actuators, A **332**, 113163 (2021).
33. V. Sai, T. Kundu, and S. Mukherji, "Novel U-bent fiber optic probe for localized surface plasmon resonance based biosensor," Biosens. Bioelectron. **24**(9), 2804–2809 (2009).
34. J. N. Dash, N. Negi, and R. Jha, "Graphene oxide coated PCF interferometer for enhanced strain sensitivity," J. Lightwave Technol. **35**(24), 5385–5390 (2017).
35. P. Ganesan, R. Kamaraj, and S. Vasudevan, "Application of isotherm, kinetic and thermodynamic models for the adsorption of nitrate ions on graphene from aqueous solution," J. Taiwan Inst. Chem. Eng. **44**(5), 808–814 (2013).
36. J. N. Dash, S. Dass, and R. Jha, "Microfiber Assisted Highly Birefringent PCF-Based Interferometric Sensors," IEEE Sensors J. **17**(5), 1342–1346 (2017).